Impact of Core Relaxation on the Asymmetry Parameter in Photoionization of Spin-Orbit Split Components of the Xenon 3d Subshell

K. P. R. V. Silva[1], C. R. Munasinghe[2], S. T. Manson[3]

[1]*Department of Physics, Faculty of Applied Sciences, University of Sri Jayewardenepura*
[2]*Department of Physics, Faculty of Science, University of Colombo*
[3]*Department of Physics and Astronomy, College of Arts and Sciences, Georgia State University*

rasadi@phys.cmb.ac.lk

1. ABSTRACT

Photoionization of the Xe 3d subshell, split into $3d_{5/2}$ and $3d_{3/2}$ by spin-orbit interaction, highlights the interplay of interchannel coupling and core relaxation effects. These mechanisms impact the angular distribution asymmetry parameter, crucial for modelling heavier atoms. Core relaxation involves reconfiguration of the residual ion's electrons after ionization, modelled more accurately by the Relativistic Random Phase Approximation with Relaxation (RRPA-R). Unlike the older RRPA, which uses only the ground state for all its calculations, even after the event of photoionization. RRPA-R incorporates both the initial ground state and the relaxed residual state, yielding more realistic angular distributions near the 3d photoionization threshold.

RRPA-R also better captures the Spin-Orbit Interaction Activated Interchannel Coupling (SOIAIC) effect, smoothing predictions of asymmetry parameter variations like the secondary peak for Xe $3d_{5/2}$. These findings show that interchannel coupling and core relaxation significantly reshape asymmetry near thresholds, improving theoretical models of atomic photoionization. Further refinement is needed for heavier systems.

2. INTRODUCTION

Atomic physics examines the properties and interactions of individual atoms. In this study, we focus on closed-shell atoms like Xenon, which are heavy enough to show relativistic effects. Due to relativistic spin-orbit interaction, the Xe 3d subshell splits into $3d_{5/2}$ and $3d_{3/2}$ components. This study examines the angular distribution asymmetry parameter of Xe 3d photoionization, an indicator of sensitive effects in well-modelled atomic photoionization.

$$\frac{d\sigma_{nl}}{d\Omega} = \frac{\sigma_{nl}}{4\pi}[1 + \beta P_2(\cos\theta)] \quad (1)$$

The asymmetry parameter, $\boldsymbol{\beta}$, is an energy-dependent quantity of the resulting photoelectron spectrum. Here, $\boldsymbol{\sigma_{nl}}$ is the cross-section of the subshell $\boldsymbol{n, l}$, and $\boldsymbol{P_2}$ is the

2nd-degree Legendre Polynomial. The angle $\boldsymbol{\theta}$ represents the photoelectron direction [1].

It should be noted that photoionization calculations become computationally expensive when done for higher-Z atoms. This is due to the many more electron-electron interactions that are possible with increasing electrons. This is why Xe was chosen to extensively test and examine these effects; it is among the lowest-Z closed-shell atoms to exhibit significant relativistic effects and Spin-Orbit Interaction Activated Interchannel Coupling (SOIAIC) effects [2].

Two significant effects are examined. First is core relaxation, where after photoionization, the residual core rearranges to reach a total energy minimum, changing the potential under which the photoelectron travels and the allowed final state continuum wavefunctions. The second effect is SOIAIC, where the larger $3d_{3/2}$ cross-section mixes with the smaller $3d_{5/2}$ cross-section around 705-710 eV, causing a small hump in the $3d_{3/2}$ beta variation around 703 eV.

This study investigates core relaxation and interchannel coupling (configuration interaction in the continuum) effects on angular distribution by measuring the variation in the beta parameter.

While the primary goal of fundamental atomic physics research is to further our understanding of atomic structure and dynamics [6, 7], it is also useful in fields such as condensed matter physics, astrophysics and plasma physics. In the case of this study in particular, as we gain a better understanding of how the angular distribution of photoelectrons changes with incident energy, it is relevant to applications where there is photoemission from a large number of atoms in free space. This includes practical applications such as lasers and plasma physics.

3. BACKGROUND

Initial experiments by Becker and his group were done in 1989 to examine the Beta parameter variation in Xenon 3d Photoionization [8]. However, these studies were done at high energy ranges far from the 3d thresholds. Therefore, Kivimäki and his group noted the need for sensitive near-threshold energy region data for Xe 3d photoionization [9]. Thus, they made many measurements with small increments in energy to examine the very sensitive character of photoionization at near-threshold energy ranges.

It was seen that there was a large mismatch between the data of Becker and Kivimäki at near-threshold energy ranges. Various theoretical calculations were conducted and showed support for Kivimäki's careful studies in this region. Therefore, it was necessary to use modern methods to re-examine Becker's data for the high-energy region. Owing to the perfect polarization of the x-ray free-electron laser (XFEL) and two-dimensional momentum imaging capability, Minemoto and his group used limited beam-time to investigate the Beta variation for Xe 3d photoionization at two energy

points: 750 and 800 eV [1]. They roughly coincide with the high energy variation in the older experimental results of Becker but there are only two points of experimental data.

Several methods have been developed for modelling beta parameter calculations [2], [3], [4], [5]. But there is a significant gap still exists between these models and experimental data for the beta parameter variation in Xe 3d photoionization at both near-threshold and higher energies.

Moreover, the computationally efficient Relativistic Time-Dependent Density Functional Theory (RTDDFT) method which was used in recent work [1] is not as reliable of a method to model sensitive photoionization effects.

Therefore, this work aims to use the much more reliable and accurate RRPA-R method, which had not been used to study the Xe 3d Beta variation, to better understand this discrepancy.

4. THEORY

4.1 Wavefunction Calculations

There are two kinds of electron wavefunctions that are dealt with in these calculations. The starting point of the calculations are the discrete orbital wavefunctions. They describe the electronic configuration of an atom. When an electron is lost due to photoionization, core relaxation is the process of discrete orbital wavefunction rearrangement.
Core relaxation itself only occurs via electron rearrangement channels that are allowed under the Electric Dipole Approximation, which is valid in the energies involved in the present work [4].

The next type of wavefunctions that are calculated are the continuum wavefunctions of the free electron(s). These are the wavefunctions that describe photoelectrons and whose probability depends specifically on their energetic overlap with the discrete orbital being photoionized. That is the probability for the specific photoionization to occur.

The Multi-Configuration Dirac-Fock (MCDF) and Dirac-Fock (DF) programs calculate the discrete orbital wavefunctions by finding an electronic configuration that is a self-consistent field. A self-consistent field is one where the electron wavefunctions are such that they are stable under the net electric field produced by them and the central nuclear potential. This is done iteratively. First, the electrons are allowed to displace in response to the net field, after which the net field is recalculated based on the new electron positions. The electrons are once again allowed to respond to the new field. This process is continued iteratively until a stable configuration with minimal electron displacement is reached. The continuum wavefunctions are also calculated under these self-consistent fields.

The power of the MCDF program is its ability to calculate relaxed wavefunctions according even when a hole is placed at a specified orbital. This hole is placed in the appropriate spin-orbit split component undergoing photoionization. The DF program on the other hand, is only able to calculate ground state wavefunctions. Therefore, the RRPA-R method uses the MCDF program while the RRPA method uses the DF program.

4.2 Verifying Wavefunction Calculations

The MCDF program also produces the total energies of the atom, before and after photoionization. The difference between these ground state and relaxed state energies are used to calculate photoionization thresholds. In the DF program however, photoionization thresholds are defined as the energy required to ionize an electron with a kinetic energy such that its total energy vanishes only at an infinite distance away from the ground state of the atom.

These two methods of calculating photoionization thresholds can be compared with the experimental values of photoionization thresholds. It has been noted that thresholds calculated using the MCDF program are much closer to the experimental values than those of the DF program. This serves as a first verification that core relaxation is an important consideration in modelling atomic physics.

4.3 Modelling Dynamics

The RRPA-R and RRPA methods require the photoionization thresholds and channels in consideration as inputs. Afterwards, as highlighted earlier, the probabilities of the continuum final state wavefunctions are calculated alongside their angular distributions. Prior to the event of photoionization, the RRPA-R method is identical to the RRPA method. After photoionization however, the situation is different. In RRPA-R, core relaxation is taken into consideration by calculating the final state continuum wave function under the potential of the relaxed residual ionic core which gives us dynamics for the photoelectron more accurately.

In the case of RRPA however, the final state continuum wave is calculated using potential due to the unrelaxed ground state atomic potential. These methods include relativistic effects in an ab initio manner.

The RRPA-R method's accuracy is verified by ensuring that the solutions obtained by the length and velocity forms of the program's results agreed to within 5% [5]. Smaller energy increments were chosen nearer to the threshold due to sensitive effects in that energy region.

As RRPA-R includes both core relaxation and interchannel coupling effects, it is expected to more accurately reproduce the otherwise elusive SOIAIC effect and other sensitive effects compared to previous models.

4. RESULTS AND DISCUSSION

Figure 1 shows RRPA-R calculations for Xe $3d_{5/2}$ beta variation compared to the theoretical RRPA and RTDDFT models, along with the experimental data of Becker, Kivimäki and Minemoto's groups.

It is notable that RRPA results has been shifted significantly by about 20 eV. This shift is due to the change in how the threshold values are calculated. It can be seen that RRPA-R matches the steep experimental dip just after the threshold, demonstrating that including core relaxation is very critical for correctly calculating threshold values.

In the higher energy region (> 770 eV), it can be seen that there is a somewhat consistent gap between the experimental data and theoretical models. There is not much of a difference between the theoretical models. This is because at high energies, the 3d to *f* channel dominates and interchannel coupling is less significant. This means that all the models will tend to the statistical value (0.8) corresponding to the 3d to *f* photoionization channel.

The experimental data shows a peak in beta at about 695 eV and a small secondary "hump" in the 700 eV range. The secondary hump is due to the SOIAIC effect, which occurs owing to the interchannel coupling between the $3d_{5/2}$ and $3d_{5/2}$ photoionization channels.

In the near threshold region, RRPA calculations show two distinct sharp peaks separated by a sharp dip, with the secondary peak at higher energy (~705 eV) being taller than the lower energy peak (~711 eV). Clearly the SOIAIC effect is grossly overemphasized in the RRPA calculation. In addition, since core relaxation is not included in RRPA, the energy scale is somewhat too high by about 8 eV.

In contrast, RRPA-R shows a broad, smooth peak around 690 eV, followed by a smaller hump near 703 eV, without any dip in-between. This overall shape matches the qualitative nature of the secondary peak that can be observed experimentally. However, a significant quantitative gap exists between the theoretical and experimental trends in this region.

As the secondary hump (~703 eV) in Xe $3d_{5/2}$ corresponds to the peak in Xe $3d_{3/2}$ cross-section, we can confirm that the observed secondary hump is due to the SOIAIC effect. Therefore, the difference in the behaviour of the secondary hump in the RRPA trend is due to the difference in the assumptions of the models. The most significant difference being the final state wavefunction being calculated differently by choosing to use the ground state instead of a completely relaxed ionic core as is done in RRPA-R. Aside from the energy shift, the difference in the two calculated results is only significant in the energy region where interchannel coupling is important. Thus, it is evident that core relaxation is essential for accurately calculating the interchannel coupling and, consequently, the SOIAIC effect [2].

Since the RRPA and RRPA-R betas hardly differ away from the region where interchannel coupling is not important, it is further evident that the continuum wave functions themselves are not greatly affected by the relaxation. Therefore, it must be that the relaxed discrete wave functions themselves that cause the interchannel coupling matrix elements to be affected strongly by relaxation.

Fig. 1 shows that there is still a small discrepancy between experimental and RRPA-R betas, which indicates that something is still missing from the theory. Our guess is that the omission of photoionization-plus-excitation channels, final-state two-particle, two-hole channels, are responsible. The inclusion of interchannel coupling with these channels could well alter the theoretical beta by the small amount needed to bring it into closer agreement with the experimental data.

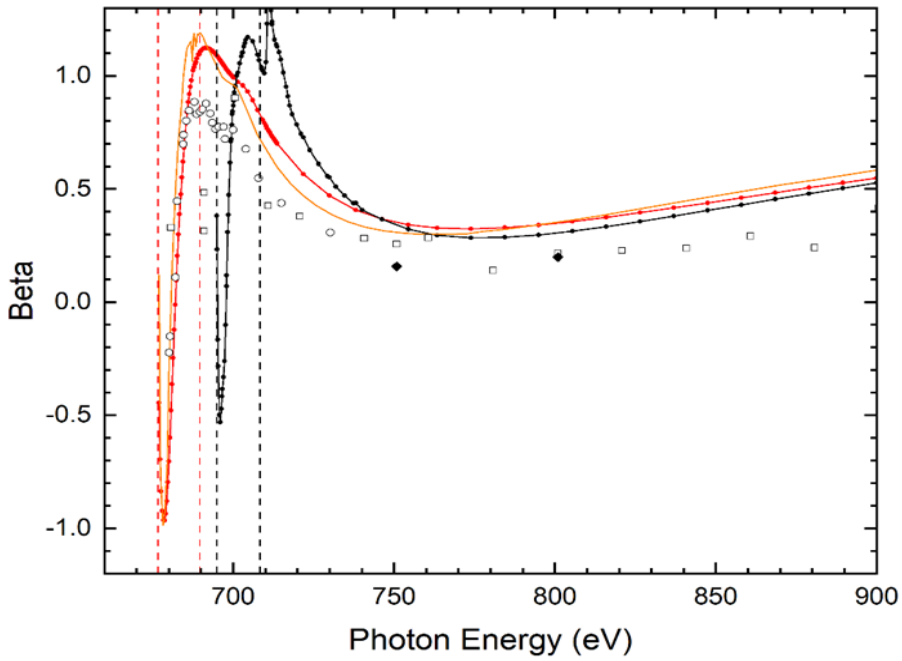

Figure 1. Beta variation in Xe $3d_{5/2}$ photoionization; Red-dots, present work (RRPA-R); Black-dots, present work (RRPA); Orange line, RTDDFT model, [1]. Experimental results: Open squares [8]; Open circles [9]; Closed diamonds [1]. Vertical dashed lines: Red, RRPA-R thresholds ($3d_{5/2}$ threshold = 676.7 eV and $3d_{3/2}$ threshold = 689.7 eV); Black, RRPA thresholds.

The effect of the central potential is softened further due to the rearrangement of the total potential in the relaxed electron cloud. This leads to the observed screening effects. Further, the SOIAIC effect is another consequence of quantum mechanical effects that occur in heavier atoms due to the mixing of cross-sections.

5. CONCLUSION

Including core relaxation is crucial as it shows both quantitative and qualitative effects, including significant screening and more accurately modelled SOIAIC effects. This is important in atomic physics as these effects are important considerations in more relativistic, heavier atoms. Therefore, it is important to understand how these dynamical effects explain experimental work that is being conducted on still heavier atoms.

Further validation is needed by examining other photoionization parameters for similar screening effects due to relaxation. Despite including core relaxation, there remains a small gap between the present model and experimental results, probably due to the omission of final-state two-particle, two-hole photoionization channels in the RRPA-R calculations. Although two-particle, two-hole interactions are included in the initial state in RRPA-R calculations, there is no way to include them directly in the final state. It might be possible to treat these final-state interactions via perturbation theory.

6. REFERENCES

[1] Minemoto, S., Teramoto, T., Majima, T., Mizuno, T., Mun, J. H., Park, S. H., Kwon, S., Yagishita, A., & Toffoli, D. (2021). *Photoelectron angular distribution studies for two spin–orbit-split components of Xe 3d subshell: a critical comparison between theory and experiment.* J. Phys. B: At. Mol. Opt. Phys., 54(10), 105003. https://doi.org/10.1088/1361-6455/abf7ce.

[2] Manson, S. T. (1976). Atomic Photoelectron Spectroscopy, Part I. In L. Marton (Ed.), Advances in Electronics and Electron Physics (vol. 41, pp. 73–111). Academic Press. https://doi.org/10.1016/S0065-2539(08)60398-4.

[3] Munasinghe, C. R., Deshmukh, P. C., & Manson, S. T. (2022). Photoionization branching ratios of spin-orbit doublets far above thresholds: Interchannel and relativistic effects in the noble gases. Phys. Rev. A, 106(1), 013102. https://doi.org/10.1103/PhysRevA.106.01310.

[4] Kutzner, M., Radojević, V., & Kelly, H. P. (1989). Extended photoionization calculations for xenon. Phys. Rev. A, 40(9), 5052–5057. https://doi.org/10.1103/PhysRevA.40.5052.

[5] Johnson, W. R., Lin, C. D., Cheng, K. T., & Lee, C. M. (1980). Relativistic Random-Phase Approximation. Phys. Scr., 21(3–4), 409. https://doi.org/10.1088/0031-8949/21/3-4/029.

[6] Banerjee, S., Deshmukh, P. C., Kheifets, A. S., & Manson, S. T. (2020). Effects of spin-orbit-interaction-activated interchannel coupling on photoemission time delay. Phys. Rev. A 101(4), 043411. https://doi.org/10.1103/PhysRevA.101.043411.

[7] Radojević, V., Davidović, D. M., & Amusia, M. Y. (2003). Near-threshold photoionization of the Xe 3□ spin-orbit doublet: Relativistic, relaxation, and intershell interaction effects. Phys. Rev. A 67(2), 022719. https://doi.org/10.1103/PhysRevA.67.022719.

[8] Becker, U., Kerkhoff, H. G., Kupsch, M., Langer, B., Szostak, D. & Wehlitz, R., (1987). PHOTOIONIZATION QF XENON WITH SOFT X-RAYS. J. Phys. Colloq. 48(1), C9-497. https://doi.org/10.1051/jphyscol:1987980.

[9] Kivimäki, A., Hergenhahn, U., Kempgens, B., Hentges, R., Piancastelli, M. N., Maier, K., Rüdel, A., Tulkki, J. J., & Bradshaw, A. M., (2000). Near-threshold study of Xe 3□ photoionization. Phys. Rev. A 63(1), 012716. https://doi.org/10.1103/PhysRevA.63.012716.